Global Change Biology (2007) **13,** 2361–2378, doi: 10.1111/j.1365-2486.2007.01417.x

The response of an Eastern Amazonian rain forest to drought stress: results and modelling analyses from a throughfall exclusion experiment

R. A. FISHER*[1], M. WILLIAMS*, A. LOLA DA COSTA†, Y. MALHI‡, R. F. DA COSTA§, S. ALMEIDA¶ and P. MEIR*

*School of GeoSciences, University of Edinburgh, Edinburgh, UK, †Universidade Federal do Pará, Belém, Pará, Brazil, ‡Centre for the Environment, University of Oxford, Oxford, UK, §Universidade Federal de Campina Grande, Paraíba, Brazil, ¶Museu Paraense Emilio Goeldi, Belém, Pará, Brazil

Abstract

Warmer and drier climates over Eastern Amazonia have been predicted as a component of climate change during the next 50–100 years. It remains unclear what effect such changes will have on forest–atmosphere exchange of carbon dioxide (CO_2) and water, but the cumulative effect is anticipated to produce climatic feedback at both regional and global scales. To allow more detailed study of forest responses to soil drying, a simulated soil drought or 'throughfall exclusion' (TFE) experiment was established at a rain forest site in Eastern Amazonia, Brazil, for which time-series sap flow and soil moisture data were obtained. The experiment excluded 50% of the throughfall from the soil. Sap flow data from the forest plot experiencing normal rainfall showed no limitation of transpiration throughout the two monitored dry seasons. Conversely, data from the TFE showed large dry season declines in transpiration, with tree water use restricted to 20% of that in the control plot at the peak of both dry seasons. The results were examined to evaluate the paradigm that the restriction on transpiration in the dry season was caused by limitation of soil-to-root water transport, driven by low soil water potential and high soil-to-root hydraulic resistance. This paradigm, embedded in the soil–plant–atmosphere (SPA) model and driven using on-site measurements, provided a good explanation ($R^2 > 0.69$) of the magnitude and timing of changes in sap flow and soil moisture. This model-data correspondence represents a substantial improvement compared with other ecosystem models of drought stress tested in Amazonia. Inclusion of deeper rooting should lead to lower sensitivity to drought than the majority of existing models. Modelled annual GPP declined by 13–14% in response to the treatment, compared with estimated declines in transpiration of 30–40%.

Keywords: Amazonia, drought, hydraulic conductivity, rain forest, sap flow, soil water, SPA model, stomatal conductance, throughfall exclusion, water relations

Received 10 April 2006; revised version received 6 April 2007 and accepted 12 April 2007

Introduction

Most global climate models predict that increasingly El Niño-like climate conditions will cause reduced rainfall over Eastern Amazonia (Cubasch *et al*., 2001). Cox *et al*. (2000, 2004) suggested that rainfall over Amazonia may be reduced as much as 65% by 2100, and that this would cause large emissions of carbon dioxide (CO_2) from the Amazon basin, associated with forest dieback. These emissions, in turn, would accelerate the rate of climate change. More recent analyses using several coupled climate and carbon cycle models indicate that over the next 100 years, the net feedback between the biosphere and atmosphere is likely to be positive, with the biosphere adding between 20 and 200 ppm to atmospheric CO_2 concentrations by 2100 (Friedlingstein *et al*., 2006). The majority of the model simulations conducted by

Correspondence: R. A. Fisher, fax +44 114 222 0002, e-mail: rosie.fisher@sheffield.ac.uk

[1]Present address: Department of Animal and Plant Sciences, University of Sheffield, Sheffield, UK.

Friedlingstein *et al*. (2006) predict a major decline in land carbon storage, located in tropical forests and the Amazon basin in particular, in response to climatic drying. However, the link between reduced rainfall and altered ecosystem gas exchange is poorly understood, and gives rise to major uncertainties in these model predictions (Nepstad *et al*., 1994; Potter *et al*., 1998; Prentice & Lloyd, 1998; Tian *et al*., 1998; Avissar & Nobre, 2002; Asner *et al*., 2004; Betts *et al*., 2004; Cowling *et al*., 2004; Cox *et al*., 2004; Gash *et al*., 2004; Huntingford *et al*., 2004; Levy *et al*., 2004; Werth & Avissar, 2004; Meir *et al*., 2006).

Uncertainty in predictions of the response of Amazonian forest gas exchange to drought is driven by two factors, the absence of appropriate data and a lack of process level understanding of water limitation in forests. Firstly, in several studies of gas exchange by tropical forests made using the eddy covariance technique (Carswell *et al*., 2002; Saleska *et al*., 2003; da Rocha *et al*., 2004; Goulden *et al*., 2004; Loescher *et al*., 2005), only one study detected a response of ecosystem-scale gas exchange to reduced water availability, at Manaus, in central Amazonia, during a single non-ENSO year (Malhi *et al*., 1998, 2002) and five studies have shown no limitation. The limited time frame and absence of complete physiological auxiliary data sets at the Manaus site mean that it was difficult to assess the exact causes of gas exchange limitation (Williams *et al*., 1998). Secondly, at present, all vegetation gas exchange models used at the ecosystem scale employ simple empirical relationships between soil moisture status and stomatal conductance or gas exchange to simulate forest drought responses (Melillo *et al*., 1993; Foley *et al*., 1996; Essery *et al*., 2002; Werth & Avissar, 2004; Woodward & Lomas, 2004). This means that even locally parameterized versions of vegetation gas exchange models have been unable to correctly predict the ecosystem drought response observed at Manaus (Harris *et al*., 2004).

To address the first problem of data availability, a 'throughfall exclusion' (TFE) experiment was constructed at Caxiuanã, in Eastern Amazonia, where rainfall was excluded from the soil over a 1 ha experimental plot. Two years of tree water use (sap flow) and 3 years of soil moisture data were collected in both the experimentally manipulated plot and an adjacent 'control' plot. These data quantified how the forest responded to drier soil conditions than those concurrently experienced in the control plot.

To facilitate improvements in process-level understanding, we investigated whether the sap-flow and soil moisture data support the paradigm of forest water limitation embedded in the soil–plant–atmosphere model (SPA) (Williams *et al*., 1996, 2001b). SPA is unique among ecosystem gas exchange models because of its explicit modelling of soil-to-leaf water transport. Two key assumptions control the responses to hydraulic stress in SPA. First, the model assumes that stomatal conductance (g_s) is controlled so that CO_2 uptake is maximized, while simultaneously preventing leaf water potential (Ψ_l) from dropping below a critical minimum value (Ψ_{crit}). Testing this assumption, Fisher *et al*. (2006) found that detailed simultaneous diurnal ecophysiological measurements of tree hydraulics (g_s, sap flow and Ψ_l) were consistent with the mechanism of stomatal conductance embedded in the SPA model across a wide range of soil moisture conditions. It is not known which plant mechanism signals water stress to stomata (Dewar, 2002; Buckley, 2005); however, several experimental studies support the hypothesis that Ψ_l cannot drop below a critical value (Tyree & Sperry, 1988, 1998; Hacke *et al*., 2000; Mencuccinni & Comstock, 2000; Hubbard *et al*., 2001; Sperry *et al*., 2002; Chapotin *et al*., 2006). Several previous modelling analyses have assumed that control of Ψ_l above Ψ_{crit} is necessary to avoid xylem damage via embolism (Sperry *et al*., 1998; Magnani *et al*., 2000; Tuzet *et al*., 2003; Katul *et al*., 2003). In addition, Dewar (2002) concluded that, while other mechanisms may play some role in regulating g_s, it was not possible to explain the observed dynamics of Ψ_l and g_s without invoking a mechanism which prevents Ψ_l decreasing below a minimum value. If stomata do function to maintain Ψ_l above Ψ_{crit}, this leads to a situation whereby, under extreme hydraulic stress, evapotranspiration is governed by the rate of supply of water from the soil to the leaf.

Soil-to-leaf water supply is driven by the soil-to-leaf water potential gradient and the total soil-to-leaf hydraulic resistance (R). Tree-scale measurements at the Caxiuanã site (Fisher *et al*., 2006) and modelling studies at Manaus (Williams *et al*., 1998) found that changes in water supply were dominated by changes in R, not water potential gradient. R is the sum of several hydraulic resistances, but it is not clear which of these is dominant under drought stressed conditions (Sperry *et al*., 1998, 2002; Williams *et al*., 1998, 2001b). Fisher *et al*. (2006) found that the belowground hydraulic resistance (R_{bg}) was the dominating resistance in the dry season, and that aboveground plant xylem resistance (R_{ag}) did not change seasonally. R_{bg} consists of both soil-to-root and root xylem resistances in series. The second assumption employed by the SPA model is that the temporal dynamics of soil-to-leaf water supply are dominated by changes in soil-to-root water transport (movement of water through the soil matrix to the root surface), not by changes in the hydraulic conductivity of the plant xylem. The plant xylem resistances are kept constant while the soil-to-root resistance is estimated from rooting density and soil hydraulic properties. Data

on soil hydraulic properties have been collected at this site (Fisher *et al*., 2007) and allow the detailed parameterization of this mechanism.

Some studies have previously considered the simultaneous impacts of changes in both soil hydraulic resistance and xylem hydraulic resistance, due to embolism (Sperry *et al*., 1998; Katul *et al*., 2003). However, these studies only considered equilibrium scenarios. Here, the aim is to generate dynamic predictions of plant water use. To implement a dynamic model of xylem embolism would require the implementation of multiple parameters defining root and shoot xylem vulnerability curves, xylem cavitation and repair processes. The assumption that *only* soil hydraulic resistance and *not* xylem resistance varies through time is therefore the most simple process-based mechanism by which low soil water may exert control over canopy water use.

Together, these two assumptions, of a critical minimum leaf water potential and variable soil-to-root water transport, form a paradigm for the mechanism underlying tree responses to drought stress. This paper investigates how much of the observed variation in water use can be explained via this paradigm. Our approach here is to use independently measured data to provide parameters for a process model. Without any optimization, the model is compared against multiple independent time-series data. The model is used to test understanding of the dynamics of the coupled SPA system, and thus, estimate the model's predictive power. This paper is novel in that we have (1) collected data on water relations of soil and plants under varied conditions in a rain forest, and (2) developed a detailed model of how soil–plant–water relations are coupled. In this analysis, consistency between process representation and observation was investigated to provide a basis for reliable prediction.

The SPA model was also used to investigate the implications of the rainfall exclusion for carbon uptake. It is not possible to measure forest carbon uptake over a 1 ha area using the eddy covariance technique, but water and CO_2 exchange are linked via stomatal conductance (Wong *et al*., 1979). Therefore, the model of stomatal conductance, which is verified against water use data, can be used as a means to predict the impact of the soil moisture deficit on canopy photosynthesis, using measured photosynthetic parameters. This model-data synthesis is used to address two key questions.

1. Are the observed seasonal changes in forest water use consistent with the paradigm that gas exchange is limited by changes in soil-to-root water supply?
2. What is the reduction in photosynthesis associated with the reduction in transpiration?

Materials and methods

Site

The experimental site is a lowland *terra firma* rainforest located in the Caxiuanã National Forest, Pará, Brazil, (1°43′3.5″S, 51°27′36″W). Mean annual rainfall is 2272 (±193) mm, with a dry season between July and December, when only 555 (±116) mm of rainfall occurs on average (data from 1999 to 2003). The soil is a yellow oxisol (Brazilian classification latosol), with a 0.3–0.4 m thick stony/laterite layer at 3–4 m depth. The soil texture (0.0–0.5 m) is 75–83% sand, 12–19% clay and 6–10% silt (Ruivo & Cunha, 2003). The site elevation is 15 m above river level in the dry season, and the water table has occasionally been observed at a soil depth of 10 m during the wet season.

To investigate the limitation of soil water on forest gas exchange in drier conditions than those normally experienced, an artificial soil drought was created using TFE. This work was carried out as part of the LBA (Large-Scale Biosphere–Atmosphere Experiment in Amazonia) Ecology programme (Avissar & Nobre, 2002). Two 100 m × 100 m plots, one control and one treatment 'TFE' plot, were established and their boundaries were trenched to a depth of 1 m to reduce the lateral flow of water. In the TFE plot, a septum comprising transparent plastic panels and plastic-lined guttering was installed at ~2 m height in December 2001, with the purpose of excluding rainfall from the soil (Fig. 1). The covering extended over 80% of the total ground area and was in place for the entire duration of the experiment (from January 2001 to December 2003) with the exception of the 4th to the 21st of November 2002, when they were removed.

Meteorology

Half-hourly meteorological data were measured using an automatic weather station located at the top (51.5 m) of a tower 1 km from the experimental plot. Rainfall was measured using a tipping bucket rainfall gauge (Campbell Scientific, Loughborough, UK) with a resolution of 0.2 mm. Atmospheric humidity was measured with an aspirated psychrometer (WP1-UM2, Delta-T Devices, Cambridge, UK). Radiation was measured with a four-component net radiometer (CNR1; Kipp and Zonen, Delft, the Netherlands) and a photosynthetically active radiation (PAR) sensor (Skye Instruments, Powys, UK). Wind speed was measured using a cup anemometer accurate to 1% (Campbell Scientific). This weather station provided 60–80% coverage over the 3 years for wet and dry bulb temperature, incoming and outgoing short-wave radiation, PAR and long-wave

Fig. 1 Throughfall exclusion installation at Caxiuanã forest. One hectare (100 m × 100 m) of plastic panels draining into aqueducts intercepts incoming rain and drains it away from the soil, causing an artificial drought. The panels cover ~80% of the ground area and were in place throughout the whole duration of the experiment, with the exception of the 4–21 November 2002, when they were removed.

radiation and wind speed. Data were collected using a datalogger (CS10X, Campbell Scientific). For all meteorological variables, measurements were made every 10 s and averaged over each 30 min period. Vapour pressure deficit (VPD) in kPa was calculated from wet and dry bulb temperatures. For the periods when no meteorological data were available, a gap-filling procedure was used (H. Iwata, personal communication). Gaps were filled for all the meteorological variables except rainfall using a mean monthly diurnal cycle, constructed from the existing data. For 2002–2003, gap filling was used for 10% of temperature data, 22% of solar radiation data and 35% of VPD data. In the case of rainfall, the gaps were filled using daily rainfall data collected from a manual weather station located in a clearing 800 m from the experimental plots, so the coverage of rainfall data was 100%. There was good agreement between the manual and automatic daily precipitation data [$R^2 = 0.87$, root mean square error of approximation (RMSE) = 0.8 mm].

Sap flow

Sap-flow rates were measured for 12 trees in each plot, chosen using size-stratified sampling, to obtain the same diameter distribution in the sample as that found in the plot. Only trees located further than 20 m from the treatment boundary were used, to minimize the impact of the boundary trenching and maximize the impact of treatment. Sap flow was measured using the trunk segment heat balance method (Cermak *et al.*, 1973, 2004) (Sap Flux Meter P4.1, Environmental Measuring Systems, Brnõ, Czech Republic). Sap flux in each tree was measured every minute and averaged over every 15 min period throughout each day. The data collection period was October 2001 to December 2003, although power problems resulted in only a few days of data being collected during the first 4 months of the collection period.

The sensors used in this technique measure sap flux velocity (kg h^{-1} m^{-1} circumference) over a sector of xylem tissue, therefore, do not require calibration for xylem depth, if the sensors (which were 30–50 mm long) penetrate horizontally through all of the active xylem tissue. Xylem depth at breast height was estimated in wood cores from 47 trees (from >35 species), ranging from 0.1 to 1.3 m in diameter, both visually, and using dye previously injected below the point of measurement. These estimates confirmed that water was not vertically transported by xylem present beyond 30 mm horizontal distance into any of the trees at breast height.

A protocol was developed to estimate the stand-scale sap flow (total sap flow per unit ground area) from the tree-scale sap flow data for each plot. Sap flow was scaled from the units of individual trees to canopy scale as follows. During the day, sap flux velocity (kg h^{-1} m^{-1} circumference) was positively correlated with tree diameter (average daytime $R^2 = 0.48$). The larger diameter trees were taller and therefore placed their leaves higher in the canopy (data not shown), where they could access more solar energy, so more transpiration occurred per unit of leaf area and by inference, per unit of sap wood area. In both plots, a census of the diameters at breast height (DBH) of all the trees >0.1 m DBH was conducted. The relationship between DBH and sap flux velocity was used to estimate the total sap flow of each tree in each plot. The sap flux velocity s (kg h^{-1}) of each tree in each experimental plot was estimated as

$$s_{t,i} = (p_t d_i + q_t) d_i, \quad (1)$$

where p_t and q_t are the slope and intercept of the estimated linear relationship between sap flux velocity (kg h^{-1} m^{-1} circumference) and diameter of the ith tree d_i (m) at time t. The stand-scale sap flow Q (kg h^{-1} m^{-2} ground area or mm h^{-1}) was then calculated as

$$Q = \frac{\sum s_{t,i} d_i}{a}, \quad (2)$$

where a is the area of the plot (m^2).

Errors for the sap flow scaling process were generated by calculating a 90% confidence interval for the value of the slope parameter p. The relative uncertainty in this value was propagated through the calculations to give the error on the stand-scale sap flow values.

Soil water content

To monitor the effect of the TFE on soil moisture, four soil access pits were constructed in each plot and time domain reflectometry (TDR) sensors identical to those described by Jipp *et al*. (1998) were placed at 0.0–0.3, 0.5, 1, 2, 3 and 5 m depths in each pit at least 1 m back from the wall of the access pit. The 0.0–0.3 m sensor was placed vertically and the other sensors were placed horizontally. The TDR sensors were monitored using a Textronix 1502C cable tester (Textronix, Richardson, TX, USA). Automatic logging was not possible with this system and soil moisture was measured manually every 10–14 days between July 2000 and December 2003. The individual waveforms produced by the cable tester were analysed using the WATTDR program (v. 3.11, Waterloo Groundwater Research, Waterloo, ON, Canada, 1996).

A gravimetric calibration of the TDR sensors was conducted by removing three 0.3 m tall $\times$ 0.15 m diameter cores of soil at 0.05–0.35 and 0.30–0.60 m depth. TDR probes were installed in the three cores; the soil was saturated and allowed to dry within a light box for 10 days. Mass and TDR waveforms were measured at gradually decreasing frequency throughout the experiment. The samples were then oven dried at 105 °C for 24 h to calculate the dry soil mass and water content derived as the difference between wet and dry mass. (Veldkamp & O'Brien, 2000). The calibration function was applied to the output of the sensors and the calibrated values were averaged over the four soil pits.

Vegetation characteristics

Leaf area index (LAI) was measured in November 2001, May 2002, November 2002, May 2003 and November 2003 at dawn using Li-Cor LAI-2000 plant canopy analysers (Li-Cor Inc., Lincoln, NE, USA). One-hundred measurements were made at every point on a marked 10 m $\times$ 10 m grid in both the control and TFE plots. Paired LAI sensors were used following a standard protocol, with one in a forest clearing, to give an image of the clear sky and the other taking measurements within the forest. Root biomass was measured using samples obtained during the construction of the soil access pits in 2001. Four pits were dug in each plot, two pits to 10 m and two pits to 5 m in the control, with four pits to 5 m in the TFE. From each of the four soil pits, all the soil extracted was sifted for roots, which were divided into diameter classes of 2–5, 5–10, 10–20 and >20 mm, then dried and weighed to find the total dry mass in each depth and diameter category.

Modelling methodology

Owing to logistical constraints, there was only one treatment and one control plot, so the TFE experiment was not replicated. Therefore, a direct statistical comparison of the two plots is not presented. Instead, we investigated whether the data from the TFE and control experiments were consistent with the paradigm that changes in soil-to-root water supply can explain the response of transpiration to soil drying, as expressed in the SPA model (Williams *et al*., 1996, 1998, 2001b). The SPA model has been successfully tested in temperate oak forest (Williams *et al*., 1996), Arctic tundra (Williams *et al*., 2000), boreal forest (Lee & Mahrt, 2004), Amazonian rain forest (Williams *et al*., 1998) and Oregon Ponderosa Pine (Williams *et al*., 2001a) ecosystems. In the last two studies, the dry season caused some limitation of gas exchange. Both analyses emphasized the importance of increased hydraulic resistance as the main factor linking soil water reductions to plant function. However, this study is the first fully parameterized test of the SPA model in a drought affected ecosystem. Details of the SPA canopy model are given in Williams *et al*. (1996) and of the SPA soil moisture model in Williams *et al*. (2001b). To avoid duplication, the description here is limited to those aspects of the model controlling drought responses.

In the SPA model, reduced soil-to-leaf water supply is linked to forest gas exchange via stomatal closure at low leaf water potential (Ψ_l) values. Ψ_l dynamics in each canopy layer, in MPa, are simulated as the balance between supply and demand

$$\frac{d\Psi_l}{dt} = \frac{\Psi_s - \rho_w g h - ER - \Psi_l}{CR}, \quad (3)$$

where Ψ_s is the soil water potential (MPa), ρ_w is the density of liquid water (kg cm^{-3}), g is gravitational acceleration (9.8 m s^{-2}) and h is the mean height (m) of the canopy layer. C is the capacitance or plant water storage (mmol m^{-2} MPa^{-1}) and R is the soil-to-leaf hydraulic resistance (m^2 s MPa mmol^{-1}). E is the rate of transpiration (mmol m^{-2} s^{-1}) calculated using the Penman–Monteith equation (Jones, 1992) for each canopy layer. g_s, an input to the Penman–Monteith equation, is calculated via an optimization routine which maximizes photosynthetic carbon uptake while preventing Ψ_l declining below Ψ_{crit} (Williams *et al*., 1996; Fisher *et al*., 2006).

The hydraulic properties determining soil-to-leaf water supply are, therefore, Ψ_s, R and C [Eqn (1)]. Ψ_s is calculated from soil water content using the van Genuchten (1980) soil hydraulics model. The sensitivity of SPA to canopy capacitance (C) is low (Williams *et al*., 1998) and has been estimated using data from

another tropical forest by Goldstein *et al*. (1998) (see Fisher *et al*., 2006 for details). Soil-to-leaf hydraulic resistance (R) is the sum of the soil-to-root (R_s), root xylem (R_{root}) and aboveground plant xylem (R_{ag}) hydraulic resistances.

Soil-to-root resistance calculations

Soil-to-root resistance for each soil layer was calculated as

$$R_s = log(\frac{\sqrt{\frac{1}{L\pi}}/r}{2\pi LK\omega g}), \quad (4)$$

where L is the total root length in the soil layer in question (m), r is the root radius (m) and K is the soil hydraulic conductivity ($m\,s^{-1}$). ω is a scaling value to convert hydraulic conductivity from $m\,s^{-1}$ to $mmol\,m^{-1}\,s^{-1}\,MPa^{-1}$.

Root length L (m) was calculated from biomass as

$$L = \frac{b}{d\pi r^2}, \quad (5)$$

where b is the root biomass (g), d is the density of the root material ($g\,m^{-3}$) and r is the mean root radius.

The total resistance of water within one soil layer $R_{t,i}$ ($m^2\,MPa\,s\,mmol^{-1}$) was found by adding the soil-to-root to the internal root transport resistance for the ith layer

$$R_{t,i} = R_{s,i} + \frac{\sigma}{b_i}, \quad (6)$$

where σ is the inverse of the conductivity of root xylem per unit biomass ($MPa\,s\,g\,mmol^{-1}$) and b_i is the total root biomass in each soil layer (g). The cumulative conductance of all the soil layers was then calculated and multiplied by the fraction of leaf area l in a given canopy layer i

$$R_{bg} = \frac{1}{\sum_{i=1}^{i=10} \frac{1}{\frac{R_{t,i}}{l}}}. \quad (7)$$

R_{bg} is then added to the aboveground resistance, $R_{ag,}$ to give the total resistance R as an input to Eqn (1).

van Genuchten soil hydraulics model

The van Genuchten (1980) model of soil hydraulics is one the most commonly used soil hydraulic models. It defines effective saturation S_e as the ratio between the water content (θ) above the residual (θ_r) and the range between the residual and saturated (θ_s) water contents (all in $m^3\,m^{-3}$)

$$S_e = \frac{\theta - \theta_r}{\theta_s - \theta_r}. \quad (8)$$

The soil water potential Ψ (MPa) is connected to the effective saturation by

$$S_e = [1 + (\alpha\psi)^n]^{1+1/n}, \quad (9)$$

where α and n are model parameters. The hydraulic conductivity K ($m\,s^{-1}$) is a function of soil water potential as follows:

$$K = K_s \frac{(1 - (\alpha\psi)^{n-1}[1 + (\alpha\psi)^n]^{-(1-1/n)^2}}{[1 + (\alpha\psi)^n]^{l_{vg}(1-1/n)}}, \quad (10)$$

where K_s is the saturated soil conductivity (K_s) and l_{vg} is a model parameter. All the model parameters (K_s, $l_{vg,}$ α, n, θ_r and θ_s) were simultaneously optimized to water potential, soil water content and soil hydraulic conductivity data for four soil depths from 0.0 to 1.0 m by Fisher *et al*. (2007). Rain water was assumed to penetrate through the entire profile via biogenic macropores, as observed in the soil moisture profile data and the infiltration experiment. Water uptake was assumed to occur only in fine roots (Tyree *et al*., 1998). The smallest root class measured was 2–5 mm, leaving some fine roots unmeasured. The measured root biomass density in the 2–5, 5–10 and 10–20 mm categories was largely similar. To estimate the fine root biomass (<2.5 mm diameter), this relationship was extrapolated and it was assumed that the fine root biomass was the same as the 2–5 mm biomass in each layer. The estimated fine root biomass was used as the input biomass for SPA.

Belowground parameterization

The SPA model calculates the belowground hydraulic resistance to water uptake ($R_s + R_{root}$) using the method of Newman (1969) where R_{root} depends on σ, the internal hydraulic resistivity of the tree roots. In the wet season, the belowground resistance at Caxiuanã was $0.19\,s\,m^2\,MPa\,mmol^{-1}$ in both plots (Fisher *et al*., 2006). It was assumed that in the wet season, belowground resistance is representative of R_{root} only as wet soil R_s is very low. σ was fixed to give wet season R_{root} of $0.19\,m^2\,MPa\,mmol^{-1}$ in each plot. R_s is estimated from root density and soil hydraulic properties. The soil hydraulic properties were measured by Fisher *et al*. (2007) using pressure plate analyses, tension infiltrometry and the instantaneous profile method (Smith & Mullins, 2000). The parameters of the van Genuchten model were fitted to the data (Table 1). For the lower soil depths (1–5 m), no hydraulic conductivity data were available, so the soil hydraulics parameters of the lowest hydraulic conductivity measurements (1 m) were used.

Table 1 Parameters of the van Genuchten Soil Hydraulics Model used in the SPA simulations taken from Fisher *et al*. (2007)

	Depth (m)			
Parameter	0.50–0.15	0.25–0.35	0.45–0.55	0.90–0.10
θ_r	0.127	0.027	0.022	0.105
θ_s	0.516	0.421	0.384	0.413
α	5.40	1.27	1.82	2.10
N	1.27	1.23	1.10	1.20
K_{sat}	1011	1545	3102	2123
l	−1.25	1.88	−1.42	−1.03

SPA, soil–plant–atmosphere.

Aboveground parameterization

The minimum water potential values measured by Fisher *et al*. (2006) had a mean value of 2.52 ± 0.75. This was very close to the value of −2.5 MPa used by Williams *et al*. (1996). Fisher *et al*. (2006) found that the average aboveground resistance (R_{ag}) was 1.79 s m^2 MPa mmol^{-1}, and did not change significantly ($P > 0.1$) between seasons, and, therefore, was defined as a constant. The parameter determining the incremental increase in photosynthesis necessary for stomata to open, *iota*, was set as 1.001, from a study using SPA by Misson *et al*. (2004), who calibrated *iota* against data from a Ponderosa Pine forest in California, USA. The SPA model predicts gross primary productivity (GPP) photosynthetic rates from estimates of g_s, which are used to generate internal leaf CO_2 concentrations. Internal leaf CO_2 concentrations, in combination with canopy layer meteorology and photosynthetic capacity measurements, are used to drive the photosynthesis model of Farquhar & Von Caemmerer (1982). The photosynthetic capacity parameters, V_{cmax} and J_{max}, were measured at different heights in the canopy (i.e. A–C_i and A–Q curves measured using a Li-6400, Li-Cor Inc., Lincoln, NE, USA; R. Lobo do Vale, personal communication).

The effect of the TFE experiment was simulated by including a dimensionless 'exclusion' parameter (ε). ε is the amount of water which is removed from the system by the rainfall exclusion panels and drained away. This process occurs after rainfall has been intercepted by the forest canopy, so

$$P_g = \varepsilon(P_t - P_i). \quad (11)$$

P_g is the rainfall reaching the ground, P_t is the total rainfall and P_i is the rainfall intercepted by the canopy and later evaporated from the leaf surface (all in mm). ε was not measured directly, but instead was estimated as 0.50 using measurements this site and data from a similar experiment in the Tapajós forest, also in eastern Amazonia.

TFE estimation

The Caxiuanã and Tapajòs TFE experiments were deliberately constructed using the same design. The structure of the Caxiuanã TFE experiment was compared with the Tapajós experiment by measuring the ground area of the forest covered by the rainfall exclusion panels (see Fig. 1). In the Caxiuanã experiment the panel coverage was 80%, close to that reported by Davidson *et al*. (2004) for the Tapajós experiment (78%). It was concluded that the Caxiuanã experiment was similar to the Tapajós experiment, since the design, materials and panel coverage were all identical. Nepstad *et al*. (2002) made physical measurements of the amount of water flowing through the drainage ditch system during rainstorms at the Tapajós forest experiment and report that, irrespective of the size of the rain storm, the TFE infrastructure excluded 50% of incoming rainfall from the soil surface. The strong linear relationship between total rainfall and rainfall reaching the ground found by Nepstad *et al*. (2002) is used to justify the linearity of Eqn (3). This value of 50% was consistent with water balance calculations using the data presented here whereby water storage = precipitation−transpiration, with no storage component. In the SPA model simulation for Caxiuanã, ε, the exclusion parameter, was set to 0.50. The interception term P_i was determined from a mechanistic model of leaf water interception within SPA. The leaf interception model fills the leaf storage until the canopy has reached saturation, after which water drains from the leaves exponentially. The evaporation of water from the surface is altered according to the altered apparent surface conductance to water (see Williams *et al*., 1996). The key parameter in this model is the canopy water storage capacity (S). Measurements of canopy interception capacity of rain forests have been made by several authors ranging from 0.74 (Lloyd & Marques, 1988), 0.93 (Dykes, 1997) to 1.15 (Schellekens *et al*., 1999) and 1.25 (Ubarana, 1996). Bruijnzeel & Wiersum (1987) report that a range of 0.8–1.2 mm was found in earlier studies. In light of these data, the canopy storage capacity in SPA was set as 1.0 mm. The sensitivity to this parameter over the 0.8–1.2 mm range was found to be low (data not shown).

The canopy parameterization is described in Table 2. All other aspects of the model, other than those mentioned in Tables 1 and 2, are the standard SPA model inputs as defined by Williams *et al*. (1996, 2001b). The SPA model was parameterized as described, and run at a 30 min resolution for 3 years from 1 January 2001 to 31 December 2003 for the control and TFE plots. The meteorological data and linearly interpolated LAI data were used to drive the model over time.

Table 2 Parameters used in the SPA model run and their origins

Parameter	Units	Control	TFE	Source
Canopy height	m	30		Measured from tower
J_{max}	$\mu mol\,m^{-2}\,s^{-1}$	43–75		Lobo do Vale *et al*. (in prep)
V_{cmax}	$\mu mol\,m^{-2}\,s^{-1}$	24–44		Lobo do Vale *et al*. (in prep)
Capacitance	$mmol\,m^{-2}\,MPa^{-1}$	2300		Goldstein *et al*. (1998)
Through fall fraction (ε)	–	1.0	0.50	Nepstad *et al* estimates
Aboveground resistance	$m^2\,MPa\,mmol^{-1}$	1.79	1.79	Fisher *et al*. (2006)
Root resistivity	$m^2\,MPa\,mmol^{-1}$	8.76	10.38	Fisher *et al*. (2006)
Iota	–	1.001	1.001	Misson *et al*.
Rooting depth	m	10	10	This paper
Ψ_{cris}	MPa	−2.52		Fisher *et al*. (2006)

Photosynthetic parameters (J_{max} and V_{cmax}) vary linearly with canopy height.
SPA, soil–plant–atmosphere; TFE, through-fall exclusion.

Measurement results

Meteorology

The meteorological measurements show seasonality in temperature, incoming short wave radiation, VPD and rainfall (Fig. 2). In each of the 3 years studied, there were high temperatures and VPD between August and November, followed by a sharp decline to wetter, cooler conditions in December. Although there is monthly variation, it is useful to split the year into the wet and dry season seasons. The wet season occurs from January to July, and the dry season from August to December. Average wet season rainfall was $9.4 \pm 11.0\,mm\,day^{-1}$. Average dry season rainfall was $3.0 \pm 9.9\,mm\,day^{-1}$. Average daytime VPD increased from 0.51 ± 0.22 kPa in the wet season to 0.72 ± 0.23 kPa in the dry season, with average daily maxima of 1.06 ± 0.34 and 1.36 ± 0.35 kPa. Mean daytime incoming short-wave radiation increased from $345 \pm 84\,W\,m^{-2}$ in the wet season to $423 \pm 74\,W\,m^{-2}$ in the dry season with maxima of 738 ± 156 and 812 ± 135. Average daily minimum temperature remained relatively constant (23.0 ± 0.6 to $23.1 \pm 1.0\,^{\circ}C$) but maximum temperature was higher in the dry season ($31.2 \pm 1.50\,^{\circ}C$) than the wet season ($29.6 \pm 1.42\,^{\circ}C$). Net radiation varied between 11.5 and $13.0\,MJ\,day^{-1}$ (annual totals of 4.1–4.2 $GJ\,yr^{-1}$ in 2001 and 2002 (Y. Malhi, personal communication).

Sap flow

Coring and dye measurements showed that the average xylem depth was 17 ± 6 mm, so the xylem rarely extended beyond 20 mm horizontally into the bole beyond the bark, irrespective of tree size. Therefore, the 30 mm long sap flow electrodes passed through all of the conductive tissue. Before the installation of the TFE experiment, the diurnal behaviour of the scaled sap flow over 5 measured days in the control and TFE plots was very similar ($R^2 = 0.89$, RMSE $= 1.38 \times 10^{-5}\,mm\,h^{-1}$), indicating that, if differences between the two plots exist, they did not affect dry season gas exchange patterns during these days. In the control plot, average sap flow in the wet season ($2.6 \pm 0.85\,mm\,day^{-1}$) was 29% lower than the average rate of sap flow in the dry season ($3.4 \pm 0.7\,mm\,day^{-1}$) (Fig. 3) suggesting that under normal climatic circumstances, water limitation did not cause a substantial decline in forest gas exchange. In the TFE plot, TFE began in November 2001, but only sparse sap flow data were available until early 2002, after the wet season had begun. The TFE plot sap flow was, on average, $0.7\,mm\,day^{-1}$ lower than the control plot sap flow until mid-August 2002. After this point, there was a very rapid reduction in TFE plot sap flow from $\sim$4 to $\sim 0.5\,mm\,day^{-1}$ within 50 days (Fig. 3). On the 4th November 2002, the panels were partially removed for a short period (marked * in Fig. 3). A large rain event (44 mm) occurred on the 16th November. Sap flow responded immediately to the pulse of rainfall, on the 17th November, increasing from 0.4 to 1.8 mm and then to 4.5 mm on the 18th November. The panels were replaced on the 21st November. The sap flow rates from the TFE plot then returned to the previous value of $\sim 0.4\,mm\,day^{-1}$. The sap flow remained low compared with the control plot until $\sim$20th March 2003, corresponding to increased soil moisture deficit. From April to June 2003, sap flow rates in both plots increased. In the TFE plot, sap flow rates declined through the 2003 dry season from July 2003 until the end of the measurement period. The sap flow of the TFE plot was on average 44% in 2002 and 41% in 2003 lower than the control plot. At the peak of the dry season in both years, sap flow in the TFE plot was 18% of that in the control, a reduction of 82%.

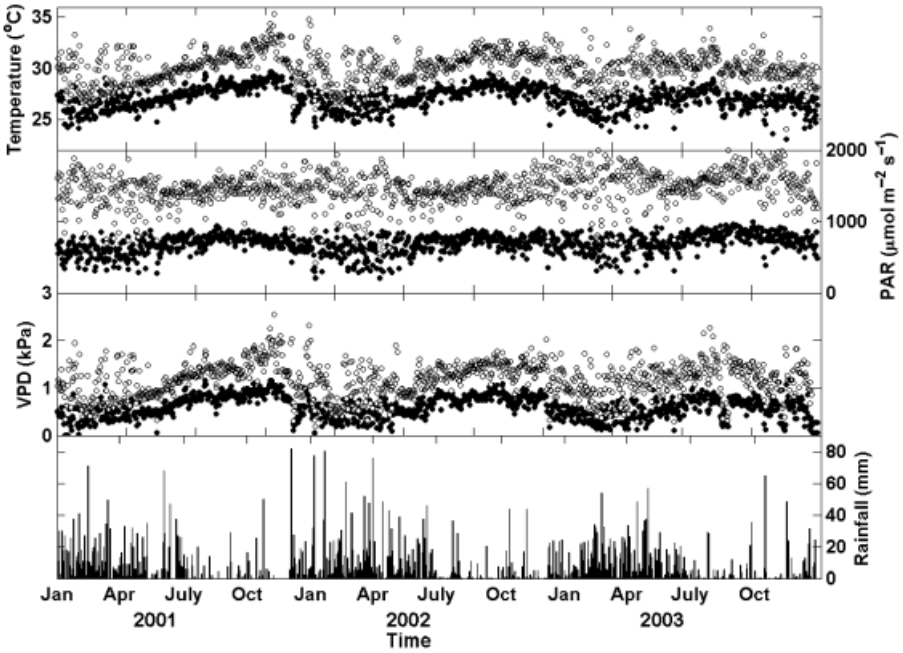

Fig. 2 Temperature, photosynthetically active radiation (PAR), vapour pressure deficit (VPD) and total daily rainfall for the period between 1 January 2001 and 31 December 2003. Filled symbols, daytime average; open symbols, daily maximum value.

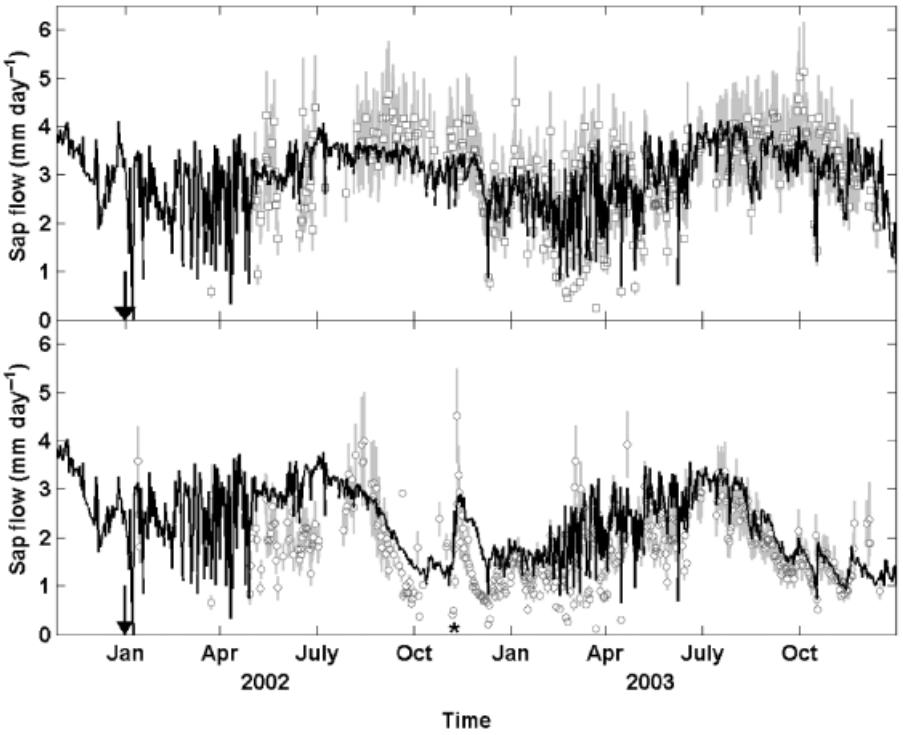

Fig. 3 Measured (symbols) and modelled (lines) stand-scale sap flow in the control (upper panel) and throughfall exclusion (lower panel) plot for 3 years using the standard SPA parameterization. Sap flow data scaled to stand-scale from a sample of 12–24 trees. The vertical arrows indicate the beginning of the throughfall exclusion. *the period when the panels were temporarily removed (explanation in text). Error bars in grey are 1 SD intervals propagated from the confidence in the relationship between tree diameter and sap flow rate. SPA, soil–plant–atmosphere.

Soil water

The best-fitting calibration between the output of the TDR sensor (t) and the gravimetric soil water content (θ, $m^3\,m^{-3}$) was $\theta = 16.61 \cdot \log\ (t) - 17.52$ ($R^2 = 0.95$, RMSE = $0.006\,m^3\,m^{-3}$). This calibration was applied to the TDR output to give θ. Soil water content in the top 3 m (Fig. 4) was initially lower in the TFE plot, but there were not significant differences (t-test, P-value > 0.05). In the control plot, θ in the top 3 m of soil varied between maxima of 860–890 mm in the wet season and minima of 570–610 mm in the dry season. Large differences between the control and TFE plot θ arose at the beginning of the 2002 wet season. The control plot rewetted from 609 to 870 mm during this time, whereas, in the TFE plot, soil water content did not exceed 645 mm during 2002 and 655 mm in 2003. The minimum soil water content in the TFE plot during the three dry seasons declined gradually from 466 mm in 2001 to 439 mm in 2002 and 398 mm in 2003.

Vegetation characteristics

LAI was initially similar in both plots and did not change until November 2002, when LAI decreased (Fig. 5). After this decline, LAI slowly increased in both plots and in November 2003 was 5.8 (SE = 0.08) and 4.6 (SE = 0.06) in the control and TFE plots, respectively. In the control plot, the total standing stock of fine root biomass integrated through the top 10 m was $865\,g\,m^{-2}$. In the TFE plot, root biomass was only measured down to 5 m for safety reasons. The root biomass declined exponentially from 0 to 5 m (Fig. 6) so an exponential model was fitted to the TFE data and used to predict the root biomass between 5 and 10 m. The form of the exponential curve was $y = 194.25\ e^{-0.66d}$ ($R^2 = 0.79$, RMSE = $34\,g\,m^{-2}$) where d is depth in metres and y is root biomass in $g\,m^{-2}$. The extrapolated total root biomass in the TFE was $567\,g\,m^{-2}$.

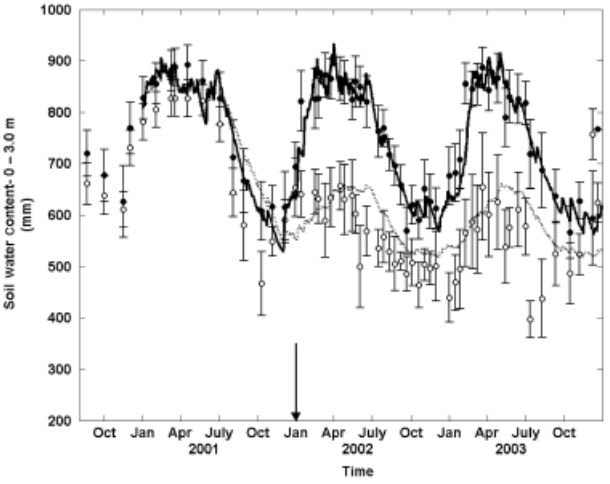

Fig. 4 Total water content (mm) in the top 3 m of soil. Measured, solid symbols (control) and open symbols [throughfall exclusion (TFE)]; Modelled, solid line (control) and dotted line (TFE). Error bars are standard errors ($n = 4$). The vertical arrows indicate the beginning of the TFE.

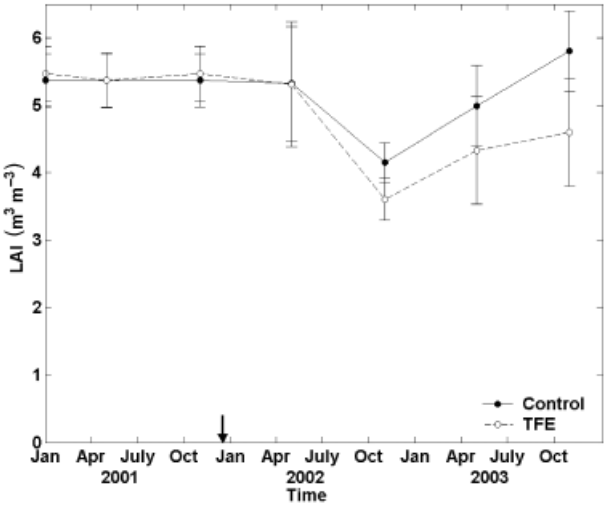

Fig. 5 Leaf area index (LAI) data for 3 years for the control (solid lines) and throughfall exclusion (TFE) (dotted lines) plots taken with LAI 2000 leaf area meter. Error bars show standard deviation where $n = 100$. Line indicates linear interpolation between data points used as model input.

Model-data comparison

In this section, we compare model predictions and data for soil moisture, soil water potential, soil-to-leaf resistance, sap flow, stomatal conductance and GPP. The SPA model provided a good explanation of the temporal changes in soil moisture content between 0 and 3.0 m (θ) that were measured in the control plot (Fig. 4) ($R^2 = 0.87$, slope = 1.02, intercept = −26 mm, RMSE = 29 mm). In the TFE plot θ simulations, R^2 was 0.68 and RMSE 64 mm (slope = 0.86, intercept = 143 mm). The reduced model fit was caused mainly by model over-prediction of θ during the dry season.

In the TFE plot, modelled dry season Ψ_s varied between −0.6 and −1.2 MPa (Fig. 7). Control plot Ψ_s varied between −0.05 and −0.2 MPa. If it is assumed that predawn Ψ_1 can be used as an estimate of Ψ_s, we can compare these values with the measurements made by Fisher *et al*. (2006) found that the gravity-corrected average predawn Ψ_1 of the TFE plot in November 2003 was -0.71 ± 0.31 MPa and of the control plot -0.17 ± 0.10 MPa.

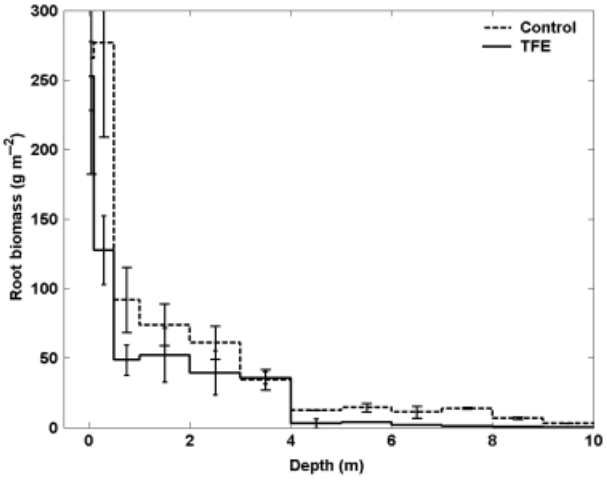

Fig. 6 Root biomass profiles for the control and throughfall exclusion (TFE) plot for roots in the smallest diameter class (2–5 mm). Error bars show standard deviation where $n = 4$ and each sample is a 1.4 m^2 soil pit. Data collected in August 2001. In the TFE plot, root biomass below 5 m was estimated from the exponential decay curve fitted to the known data. $y = 194.25\,e^{-0.66d}$, where d is depth in metres.

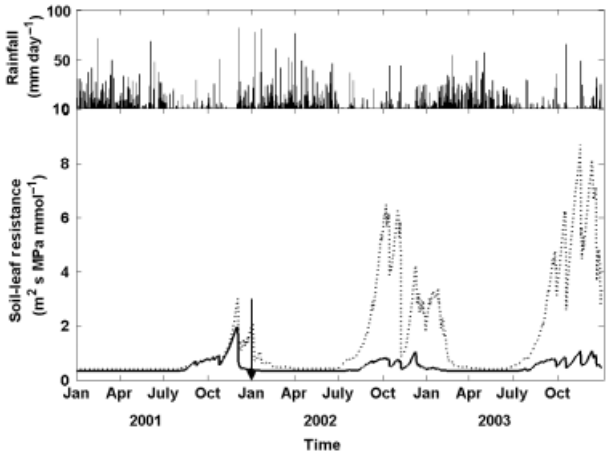

Fig. 8 Top panel, daily rainfall (mm day^{-1}); bottom panel, modelled changes in soil to leaf hydraulic resistance in the control (solid line) and throughfall exclusion (TFE) (dotted line) plots using the SPA model. All changes in soil-leaf resistance were located in the soil as the result of decreased soil hydraulic conductivity according to the equations of Newman (1969). The vertical arrow indicates the beginning of the. SPA, soil–plant–atmosphere.

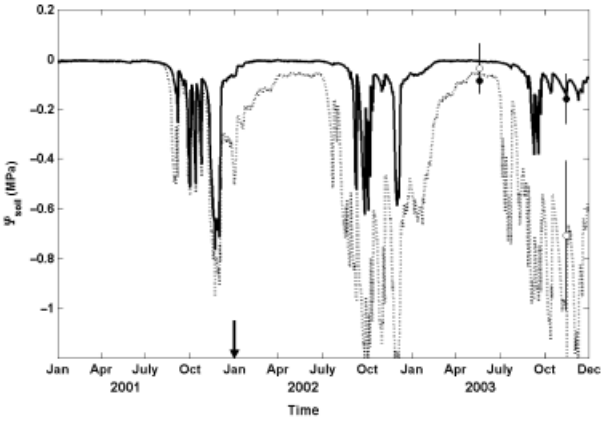

Fig. 7 Modelled time-courses of soil water potential Ψ_s for the control (solid line) and throughfall exclusion (TFE) plots. Modelled values are a weighted average over the top 1 m of soil depth. Symbols (control plot, filled; TFE plot, empty) are the predawn Ψ_l measurements, scaled for leaf height to estimate the effective Ψ_s. The vertical arrows indicate the beginning of the TFE.

The modelled reduction in θ in the TFE plot from the wet to the dry season caused a concurrent increase in the modelled soil-to-root hydraulic resistance. In the dry season, R in the TFE plot peaked at 3.0 s m^2 MPa mmol^{-1} in 2001, 6.5 s m^2 MPa mmol^{-1} in 2002 and 8.6 s m^2 MPa mmol^{-1} in 2003 (Fig. 8). The control plot showed only very slight increases in R from 1.9 s m^2 MPa mmol^{-1} in the wet season to 2.5 s m^2 MPa mmol^{-1} in the dry season. The 2003 dry season values of R measured for individual trees by Fisher *et al*. (2006) were 7.8 ± 5.9 and 3.1 ± 0.7 s m^2 MPa mmol^{-1} in the TFE and control, respectively. The model was within the 1 SD confidence limits of the data.

R^2 of the modelled vs. measured daily sap flow was 0.78 in the control and 0.69 in the TFE plot (Fig. 3, Table 3). In the control plot, where there were only small changes in the R and Ψ_s between seasons, water use was higher in the dry season than the wet season, indicating that hydraulic stress was not present in this treatment under normal rainfall. In the TFE plot, reduced soil-to-leaf water supply in the dry season was caused by low Ψ_s and high R. Limited soil-to-leaf water supply lowered modelled Ψ_l to near Ψ_{crit}. This low Ψ_l triggered reduced modelled g_s and sap flow during the dry season. The reductions in modelled sap flow were of similar timing and magnitude to those observed in the data (Fig. 3). The slopes of the model-data relationship were 1.02 and 0.82 in the control and TFE, respectively (Table 3), indicating a slight overprediction by the SPA model, especially in the control plot. Most temporal events in the observed water cycle were similar to model predictions, in particular, the response to a large rainstorm during the period when the covers were removed in November 2002, the wet to dry season transition period of 2003 and the responses to small rain storms in the 2003 dry season (Fig. 3). In the wet season of 2002, sap flow is overestimated by the model

for both plots and the onset of the drought stress is too early. During this period, there were some gaps in the meteorological data, which may have lead to these erroneous predictions. The diurnal sap flow patterns both in the wet season and in the dry season of 2003 were also well simulated (Fig. 9). R^2 values of half hourly sap flow were 0.82 and 0.75 for the control and TFE plots, respectively.

Estimated annual totals of transpiration were similar for 2001, 2002 and 2003 in the control plot (1316, 1253 and 1223 mm) but gradually decreased from year to year in the TFE plot (1258, 953 and 805 mm). The reduction in the total modelled annual sap flow of the TFE plot, compared with the control plot, was 31% in 2002 and 41% in 2003, compared with measured estimates (for the times when data from both plots were available) of 44% in 2002 and 41% in 2003. Modelled sap flow rates indicate that the control plot transpired 54–58% of the incoming rainfall in all years. In the TFE plot, 58% of the rainfall was transpired in 2001, rising to 91% in 2002 and 85% in 2003 as the rainfall was reduced. Less water was, therefore, available for drainage, and the reduced drainage would have larger scale impacts on river flow and regional hydrology. The proportion of net radiation used for transpiration was estimated as 77–82% in the control plot. In the TFE plot, the 2001 proportion was 79%, declining to 60% in 2002 and 51% in 2003 as transpiration was limited by water availability. These values only include transpired water, and do not include evaporation from leaf or soil surfaces.

Modelled daytime (06:00–18:00 hours) bulk average g_s of sun and shade leaves over all 10 canopy layers was reduced, in the TFE plot from $\sim$150 to $\sim$60 mmol $m^{-2} s^{-1}$ during both dry periods. In the TFE plot, these data closely match the average daytime stomatal conductance values directly measured at this site by Fisher *et al.* (2006), who found $g_s = 138 \pm 33$ and 63 ± 17 mmol $m^{-2} s^{-1}$ in May and November of 2003,

Table 3 Statistics of model-data comparison for sap flow and soil water content for control and through-fall exclusion (TFE) plots

Data type	Units	Statistic	Control	TFE
Sap flow	mm day^{-1}	R^2	0.78	0.69
		RMSE	0.37	0.54
		Slope	0.80	0.93
		Intercept	0.40	0.44
Soil water	$m^3 m^{-3}$	R^2	0.87	0.68
		RMSE	29	64
		Slope	1.02	0.86
		Intercept	−26	143

($R^2 = 0.87$, slope = 1.02, intercept = −26 mm, RMSE = 29 mm). In the TFE plot θ simulations, R^2 was 0.68 and RMSE 64 mm (slope = 0.86, intercept = 143 mm).
RMSE, root mean square error of approximation.

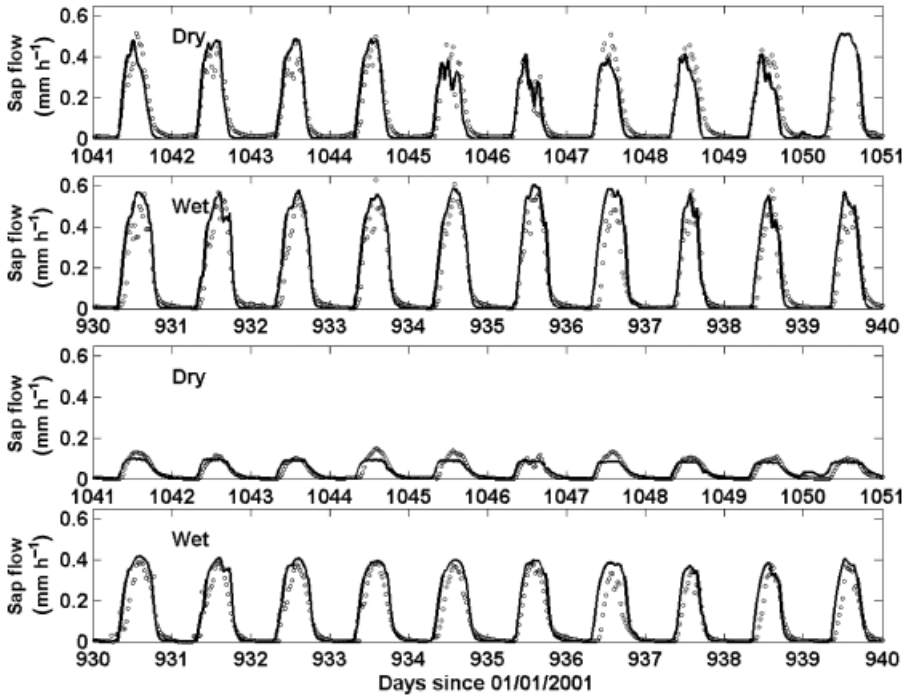

Fig. 9 Measured (symbols) and modelled (lines) half-hourly stand-level sap flow for the control plot (top two panels) and through-fall exclusion plot (bottom two panels).

respectively. In the control plot, average modelled g_s was $\sim$170 and $\sim$150 mmol m^{-2} s^{-1} in May and November 2003, compared with measured values of 141 ± 37 and 98 ± 32 mmol m^{-2} s^{-1}. The model over-predicts stomatal conductance in the control plot, but, given the variation between trees in values of g_s it is difficult to assign confidence limits to these measured values. However, there is a good model fit to sap flow data at these times, (Fig. 3), and these provide a measurement which is averaged over entire leaf populations of trees, and a greater sample size of individual trees. Reduced stomatal conductance decreased modelled GPP (Fig. 10). In the wet season, 5-day average modelled canopy GPP was very similar between plots (Fig. 10), but in the dry season, the GPP of the TFE plot was reduced to 55–60% of the GPP of the control plot, in response to a modelled draw down of internal leaf CO_2 concentration.

Estimates of maximum daily GPP using data from an eddy-covariance study also located at Caxiuanã (Carswell *et al*., 2002) yielded similar rates of maximum GPP in the wet and dry seasons, respectively, (of 27 and 29 μmol s^{-1} m^{-2}) to those predicted by the model (27 μmol s^{-1} m^{-2} for both seasons). The Carswell *et al*. data were corrected for in-canopy CO_2 storage, but not for the potential effects of CO2 advection under low u^* conditions.

Discussion

Are the observed seasonal changes in transpiration consistent with the paradigm that gas exchange is limited by changes in soil-to-root water supply?

The predictions of the SPA model were found to be broadly consistent with the observed short and long term dynamics of sap flow, soil water content, soil water potential, leaf water potential and stomatal conductance data across a wide range of soil moisture conditions. The model was able to explain 69% of the variance in sap flow and 68% of the variance in θ in the TFE plot and model residuals were 12% and 31% of the mean model sap flow. These results, therefore, provide support for the paradigm that forest water use is controlled by changes in soil to root water transport. Of the remaining 30% error in sap flow predictions, some will

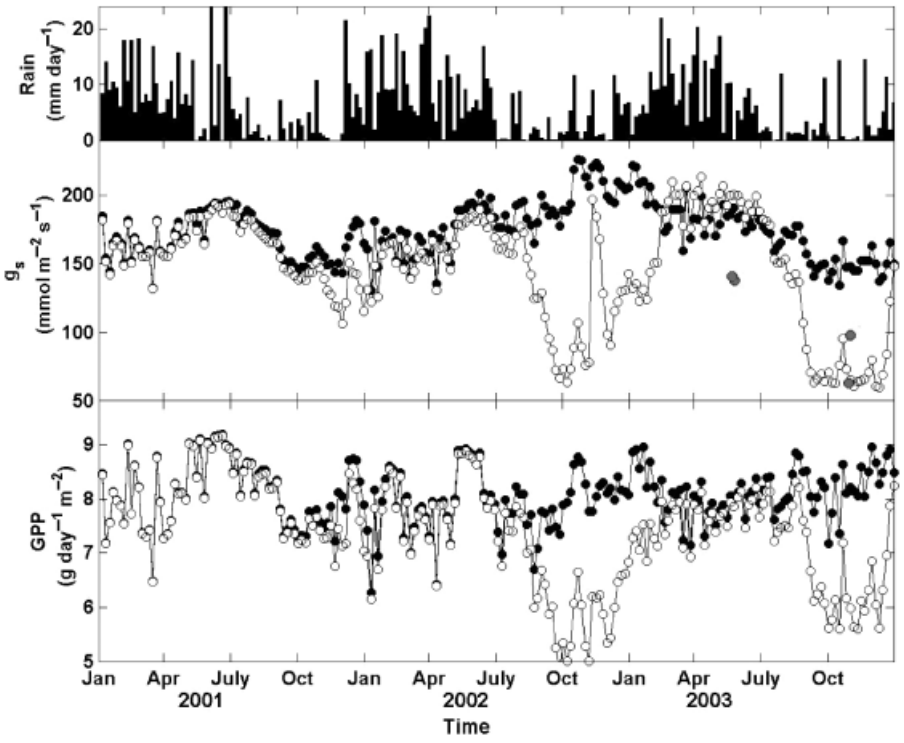

Fig. 10 Upper panel, daily rainfall (mm day^{-1}); middle panel, 5-day average daytime leaf level stomatal conductance (average of sun and shade leaf stomatal conductance per unit leaf area weighted for leaf area at 10 canopy layers between 06:00 and 18:00 hours) for the control (dotted line, open symbols) and throughfall exclusion (TFE) (solid line, filed symbols); bottom panel, simulated GPP for the control (dotted line, open symbols) and TFE (solid line, filed symbols). Five-day average values from half-hourly simulations by the SPA model. The vertical arrows indicate the beginning of the through-fall exclusion. SPA, soil–plant–atmosphere; GPP, gross primary productivity.

be attributable to measurement error, some to inaccurate model parameterizations and driving data and some to inappropriate model process representation. To assess the contribution of process representation inaccuracy in time-series analyses with multiple data sets such as these, data assimilation methods comparing model input parameter uncertainty to data uncertainty should be used (i.e. Williams *et al*., 2005). These are beyond the scope of this paper but will be the subject of future investigations.

The results found here support the idea that soil-to-root resistance exerts a large control on transpiration. In contrast, Sperry *et al*. (1998) found in a modelling analysis, that high-xylem (not soil-to-root) resistance, due to cavitation and embolism, exerted the largest control on the soil-to-leaf transport of water. Embolism was not explicitly modelled in this study, so its importance cannot be ruled out. However, Sperry *et al*. did not model conditions with rooting density as low as those found at this site. Furthermore, they predict that under conditions of lower rooting density, it is more likely that soil-to-root resistance would be the largest resistance in the soil-plant-atmosphere continuum; a view which is consistent with the results found in this study. Deep rooting may be a general feature of Amazonian soils (Nepstad *et al*., 2002) so the large vertical distribution and low density of root biomass is likely to be a common feature of rain forest ecosystems, widening the generality of these conclusions.

Several assumptions were made by the modelling approach used here. First, it was assumed that root biomass did not change through the experiment. Altered root biomass would certainly alter the soil-to-root hydraulic resistance. Presumably, the effect of drought would be to increase belowground allocation and root biomass, ameliorating the response of the forest to drought, although this effect was not evident in the sap flow data. It was also assumed that roots are evenly spread through the soil and have constant radius, and that soil properties below 1.0 m do not change substantially. It is recognized that these assumptions remain untested, however, detailed investigation into root dynamics is underway at the Caxiuanã site, which should provide insight into their importance.

In the control plot, little evidence was found of limitation of transpiration in the dry season, as gas exchange rates were substantially higher than in the wet season (Fig. 3). This finding is in common with recent satellite observations (Huete *et al*., 2006) and the majority of eddy covariance measurements of gas exchange (Carswell *et al*., 2002; Saleska *et al*., 2003; Goulden *et al*., 2004; da Rocha *et al*., 2004; Loescher *et al*., 2005) but is at odds with terrestrial ecosystem model predictions of contemporary Amazonian gas exchange (Tian *et al*., 1998; Zeng *et al*., 2005; Peylin *et al*., 2006) which predict large declines in assimilation during dry periods.

What is the reduction in photosynthesis associated with the reduction in sap flow?

Extrapolation of the estimated stomatal conductance values, using the photosynthesis model of Farquhar & von Caemmerer (1982) indicated that a 13–14% drop in GPP occurred as a result of the TFE experiment over the 2 years of the experiment, with a reduction of 40–45% during the driest periods (Fig. 10). The reductions in photosynthesis are predicted to occur in tandem with the reductions in sap flow, and were due to the (predicted) declines in stomatal conductance during the dry seasons in the TFE plot (Fig. 10). Reductions in modelled GPP were less extreme than reductions in transpiration, as transpiration is linearly related to stomatal conductance, whereas photosynthesis may be limited by a variety of other factors and thus does not respond linearly to instantaneous changes in stomatal conductance.

Modelled GPP was $3094\,g\,m^{-2}\,yr^{-1}$ in the control and $2685\,g\,m^{-2}\,yr^{-1}$ in the TFE in 2002, and $3138\,g\,m^{-2}\,yr^{-1}$ in the control and $2705\,g\,m^{-2}\,yr^{-1}$ in the TFE in 2003. The average difference in total GPP between the control and the TFE plots was 13.2% and 13.8% in 2002 and 2003, respectively. In addition, studies of carbon stocks within the TFE experiment show that stem growth in the TFE plot effectively ceased over the course of the experiment and that there was a decline in leaf area as described above. Both of these observations are consistent with a large decrease in carbon input from GPP. The impact of the treatment on net ecosystem exchange of CO_2 will be the subject of future publications (P. Meir, personal communication).

Conclusions

Measurements over 2 years in an eastern Amazonian rain forest indicate that transpiration is higher in the dry season than the wet season under normal circumstances, and there is little evidence for limitation of water use during the dry season. However, experimental TFE, removing an estimated 50% of the rainfall, caused soil drying and a resultant decrease in total sap flow of 41% with the most severe drought periods causing an 80% reduction in sap flow compared with the control. These results, which suggest that the forest is not able to withstand a 50% reduction in rainfall over 1–2 years without impacts on canopy gas exchange, are in contrast with the results of Nepstad *et al*. (2002) for their TFE experiment, located in the Tapajòs national

forest. Nepstad *et al*. measured predawn leaf water potentials over the course of 2 years and found no change in Ψ_{pd}, suggesting that the TFE did not provoke substantial drought stress in the canopy for the first 2 years, although changes were found in the dry season of the second year (Asner *et al*., 2004). There are several possible explanations for this contrast with the Caxiuanã results. Firstly, the Tapajòs experiment did not impose a continuous TFE. Instead, the panels were removed during the dry season, thereby reducing the total impact of the treatment. In addition, the Tapajòs experiment was located on a clay type soil which is known to be at least 90 m deep, and, in contrast to the Caxiuanã site, does not have a stony laterite layer, which may prevent the development of substantial deep root systems at Caxiuanã (although roots were found below this layer). The vertical extent of the root system, and the water holding capacity of the soil may, therefore, have contributed to the increased drought resilience of the Tapajòs forest, but published data is not available on either parameter to establish whether this is the case.

The experiment was designed to simulate future low rainfall conditions predicted by Cox *et al*. (2000) for Eastern Amazonia. The level of rainfall reduction experienced by both Tapajòs and Caxiuanã experiments (50%) was less than that predicted by Cox *et al*. (2000), (2004., using the HADCM3LC global climate model coupled to a dynamic vegetation model, predicted a decrease in average rainfall over the Amazon basin from 4.56 mm day^{-1} in 2000 to 1.64 mm day^{-1} in 2100, a decline of 65% over the 21st Century. However, Betts *et al*. (2004) propose that, while approximately half of this reduction is caused by changes in global climate patterns, the other half is due to feedback on rainfall from changes in vegetation cover. The feedback is both regional, via biophysical feedbacks, and global, via increases in CO_2 levels due to the die-back of Amazon forests. The parameterization of the magnitude of both feedback processes is uncertain (Harris *et al*., 2004; Huntingford *et al*., 2004) and this uncertainty formed part of the justification for this experiment. Greater confidence in modelling the Amazon-climate interaction, and hence in predicting rainfall declines, may now be achieved by assimilating results from experiments of this kind into global vegetation models (e.g. Huntingford *et al*., 2004). Different global climate models predict different rainfall scenarios over Amazonia, with the Hadley Centre models consistently producing the most severe drying over the Amazon region. However, the recently published fourth IPCC assessment report (Fig. 7; IPCC, 2007) suggests that, over large areas of Southern and Eastern Amazonia, there is agreement between GCM's that dry season rainfall will decline by 10–30%. In Northern and Central areas, there is no agreement between GCMs and in a small area of the Western Amazon, a slight increase in precipitation rates is predicted. None of these GCM simulations included dynamic vegetation models, or the impacts of land use change. On going deforestation is likely to reduce evaporation over the whole Amazon basin, even in the absence of climate change and climatic drying is likely to reduce evaporation over the Southern Amazon. These changes in vegetation cover due to climate or land use change are likely to amplify any changes in the forcing meteorology (Betts *et al*., 2004). Again, information from rainfall exclusion experiments should help inform land surface models about the likely extent of these feedback processes. However, the TFE experiment reported here only altered rainfall, and not temperature, VPD or radiation. Increases in all these factors are predicted under the warming and drying scenario, but it is not possible to experimentally test their simultaneous effects on forest physiology. Clearly, it is likely that the concomitant increases in temperature and VPD will decrease the ability of the forest to withstand low rainfall. It is only through the development of physically based models, such as SPA, that the effects of these complex changes in multiple environmental variables can be investigated.

The reductions in sap flow and soil moisture observed in this study were mainly consistent with the paradigm that changes in soil-to-root water supply are the major control of transpiration under reduced soil water conditions, as embedded in the SPA model. In combination with the verification of the model against diurnal tree physiology data by Fisher *et al*. (2006), the findings presented here imply that it is feasible to mechanistically model responses to drought by rain forest if soil hydraulic and root profile properties are known. Information on both of these ecosystem properties is very sparse in Amazonia (Tomasella & Hodnett, 1997; Nepstad *et al*., 2004), but estimation of both is possible without sophisticated measurement techniques. If improvements in understanding of the feedback between the potential future drying of the forest and the climate system are to be made, then better knowledge of the spatial variation in active rooting depth, soil water-holding capacity and soil hydraulic conductivity must be obtained. However, because these inputs to the SPA model can be measured directly, their potential ranges may be constrained using ground-based measurements, leading to greater confidence in the predictions of global models Given the potential global importance of this feedback mechanism (Cox *et al*., 2000, 2004; Friedlingstein *et al*., 2006), data collection on the ecosystem properties must be considered a priority.

Acknowledgements

This work was supported by a University of Edinburgh faculty research Scholarship, several Natural Environment Research Council (UK) research grants, a Natural Resources International Foundation Fellowship and the Elizabeth Sinclair fund (University of Edinburgh). The authors would like to thank John Grace for comments on the manuscript, Raquel Lobo do Vale and Luiz Aragão for provision of unpublished data, Alan Braga, João Athaydes and Paulo Gonçalves for field assistance and the Museu Paraense Emilio Goeldi for the use of their field station and laboratory facilities.

References

Asner GP, Nepstad D, Cardinot G, Ray D (2004) Drought stress and carbon uptake in an Amazon forest measured with spaceborne imaging spectroscopy. *Proceedings of the National Academy of Sciences, USA*, **101**, 6039–6044.

Avissar R, Nobre CA (2002) Preface to special issue on the large-scale biosphere–atmosphere experiment in Amazonia (LBA). *Journal of Geophysical Research -Atmospheres*, **107**, 8034.

Betts RA, Cox PM, Collins M, Harris PP, Huntingford C, Jones CD (2004) The role of ecosystem–atmosphere interactions in simulated Amazonian precipitation decrease and forest dieback under global climate warming. *Theoretical and Applied Climatology*, **78**, 157–175.

Bruijnzeel LA, Wiersum KF (1987) Rainfall interception of a young *Acacia auriculiformis* (A Cunn.) plantation forest in West Java, Indonesia: application of Gash's analytical model. *Hydrological Processes*, **1**, 309–319.

Buckley T (2005) The control of stomata by water balance. *New Phytologist*, **168**, 275–292.

Carswell FE, Costa AL, Palheta M (2002) Seasonality in CO_2 and H_2O flux at an eastern Amazonian rain forest. *Journal Of Geophysical Research*, **107**, 8076.

Cermak J, Deml M, Penka M (1973) New method of sap flow-rate determination in trees. *Biologia Plantarum*, **15**, 171–178.

Cermak J, Kucera J, Nadezhdina N (2004) Sap flow measurements with some thermodynamic methods, flow integration within trees and scaling up from sample trees to entire forest stands. Trees. *Structure And Function*, **18**, 529–546.

Chapotin SM, Razanameharizaka JH, Holbrook NM (2006) Water relations of baobab trees (Adansonia spp. L.) during the rainy season: does stem water buffer daily water deficits? *Plant, Cell and Environment*, **29**, 1021–1032.

Cox PM, Betts RA, Collins M, Harris PP, Huntingford CC, Jones CD (2004) Amazonian forest dieback under climate-carbon cycle projections for the 21st century. *Theoretical and Applied Climatology*, **78**, 137–156.

Cox PM, Betts RA, Jones CD, Spall SA, Totterdell IJ (2000) Acceleration of global warming due to carbon-cycle feedbacks in a coupled climate model. *Nature*, **408**, 184–187.

Cowling SA, Betts RA, Cox PM, Ettwein VJ, Jones CD, Maslin MA, Spall SA (2004) Contrasting simulated past and future responses of the Amazonian forest to atmospheric change. *Philosophical Transactions of the Royal Society of London Series B-Biological Science*, **359**, 539–547.

Cubasch U, Meehl GA, Boer GJ *et al*. (2001) Projections of future climate change. In: *Climate Change 2001: The Scientific Basis. Contribution of Working Group I to the Third Assessment Report of the Intergovernmental Panel on Climate Change* (eds Houghton JT *et al*.), pp. 525–582. Cambridge University Press.

da Rocha HR, Goulden ML, Miller SD, Menton MC, Pinto L, deFreitas HC, Figueira A (2004) Seasonality of water and heat fluxes over a tropical forest in eastern Amazonia. *Ecological Applications*, **14**, S22–S32.

Davidson EA, Ishida FY, Nepstad DC (2004) Effects of an experimental drought on soil emissions of carbon dioxide, methane, nitrous oxide, and nitric oxide in a moist tropical forest. *Global Change Biology*, **10**, 718–730.

Dewar RC (2002) The Ball–Berry–Leuning and Tardieu–Davis stomatal models: synthesis ad extension within a spatially aggregated picture of guard cell function. *Plant, Cell and Environment*, **202**, 1383–1398.

Dykes AP (1997) Rainfall interception from a lowland tropical rainforest in Brunei. *Journal of Hydrology*, **200**, 260–279.

Essery R, Best M, Cox P (2002) *MOSES 2.2 Technical Documentation*. Hadley Centre Technical Note 30. Met Office UK.

Farquhar GD, Von Caemmerer S (1982) Modelling of photosynthetic response to the environment. In: *Physiological Plant Ecology II. Encyclopedia of Plant Physiology, New Series*, Vol. 12B (eds Lange OL, Nobel PS, Osmond CB, Ziegler H), pp. 549–587. Springer-Verlag, Berlin.

Fisher RA, Williams M, Lobo do Vale R, Costa A, Meir P (2006) Evidence from Amazonian forests is consistent with isohydric control of leaf water potential. *Plant, Cell and Environment*, **29**, 151–165.

Fisher RA, Williams M, Ruivo MDL, Lola da Costa A, Meir P (2007) Evaluating climatic and edaphic controls on drought stress at two Amazonian sites. *Agricultural & Forest Meterology* (in review).

Foley JA, Levis S, Prentice IC, Pollard D, Thompson SL (1996) Coupling dynamic models of climate and vegetation. *Global Change Biology*, **4**, 561–579.

Friedlingstein P, Cox P, Betts R *et al*. (2006) Climate – carbon cycle feedback analysis: results from the C4MIP model intercomparison. *Journal of Climate*, **14**, 3337–3353.

Gash JHC, Huntingford C, Marengo JA *et al*. (2004) Amazonian climate: results and future research. *Theoretical and Applied Climatology*, **78**, 187–193.

Goldstein G, Andrade JL, Meinzer FC, Holbrook NM, Cavalier J, Jackson P, Celis A (1998) Stem water storage and diurnal patterns of water use in tropical forest canopy trees. *Plant, Cell and Environment*, **21**, 397–406.

Goulden ML, Miller SD, da Rocha HR, Menton MC, de Freitas HC, Figueira A, de Sousa CAD (2004) Diel and seasonal patterns of tropical forest CO_2 exchange. *Ecological Applications*, **14**, S42–S54.

Hacke UG, Sperry JS, Ewers BE, Ellsworth DS, Schäfer KVR, Oren R (2000) Influence of soil porosity on water use in *Pinus taeda*. *Oecologia*, **124**, 495–505.

Harris PP, Huntingford C, Gash JHC, Hodnett MG, Cox PM, Malhi Y, Araujo AC (2004) Calibration of a land-surface model using data from primary forest sites in Amazonia. *Theoretical and Applied Climatology*, **78**, 27–45.

Hubbard RM, Ryan MG, Stiller V, Sperry JS (2001) Stomatal conductance and photosynthesis vary linearly with plant hydraulic conductance in ponderosa pine. *Plant, Cell and Environment*, **24**, 113–121.

Huntingford C, Harris PP, Gedney N, Cox PM, Betts RA, Marengo JA, Gash JHC (2004) Using a GCM analogue model to investigate the potential for Amazonian forest dieback. *Theoretical and Applied Climatology*, **78**, 177–185.

Huete AR, Didan K, Shimabukuro YE *et al*. (2006) Amazon rainforests green-up with sunlight in dry season. *Geophysical Research Letters*, **33**, L06405.

IPCC. Misc: *Summary for policymakers: climate change 2007*, Fourth Assessment Report, The Physical Science Basis.

Jipp PH, Nepstad DC, Cassel DK, De Carvalho CR (1998) Deep soil moisture storage and transpiration in forests and pastures of seasonally-dry Amazonia. *Climatic Change*, **39**, 395–412.

Jones HG (1992) *Plants and Microclimate*. Cambridge University Press, Cambridge.

Katul G, Leuning R, Oren R (2003) Relationship between plant hydraulic and biochemical properties derived from a steady-state coupled water and carbon transport model. *Plant, Cell and Environment*, **26**, 339–350.

Lee YH, Mahrt L (2004) Comparison of heat and moisture fluxes from a modified soil–plant–atmosphere model with observations from BOREAS. *Journal of Geophysical Research*, **109**, D08103.

Levy P, Friend AD, White A, Cannell MGR (2004) The influence of land use change on global-scale fluxes of carbon from terrestrial ecosystems. *Climatic Change*, **67**, 185–209.

Lloyd CR, Marques A de O (1988) Spatial variability of throughfall and stemflow measurement in Amazonian rainforest. *Agricultural and Forest Meteorology*, **42**, 63–73.

Loescher HW, Gholza HL, Jacobs JM, Oberbauer SF (2005) Energy dynamics and modeled evapotranspiration from a wet tropical forest in Costa Rica. *Journal of Hydrology*, **315**, 274–294.

Magnani F, Mencuccinni M, Grace J (2000) Age related decline in stand productivity: the role of structural acclimation under hydraulic constraints. *Plant, Cell and Environment*, **23**, 251–263.

Malhi Y, Nobre AD, Grace J, Kruijt B, Pereira MGP, Culf A, Scott S (1998) Carbon dioxide transfer over a Central Amazonian rain forest. *Journal of Geophysical Research-Atmospheres*, **103**, 31.593–31.612.

Malhi Y, Pegoraro E, Nobre AD, Pereira MGP, Grace J, Culf AD, Clement R (2002) Energy and water dynamics of a central Amazonian rain forest. *Journal of Geophysical Research-Atmospheres*, **107**, 8061.

Mencuccinni M, Comstock J (2000) Stomatal responsiveness to leaf water status in common bean (*Phaseolus vulgaris* L.) is a function of time of day. *Plant, Cell and Environment*, **23**, 1109–1118.

Meir P, Cox PM, Grace J (2006) The influence of terrestrial ecosystems on climate. *Trends in Ecology and Evolution*, **5**, 254–60.

Melillo JM, McGuire AD, Kicklighter DW, Moore B III, Vorosmarty CJ, Schloss AL (1993) Global climate change and terrestrial net primary production. *Nature*, **363**, 234–240.

Misson L, Panek JA, Goldstein AH (2004) A comparison of three approaches to modelling leaf gas exchange in annually drought-stressed ponderosa pine forests. *Tree Physiology*, **24**, 529–541.

Nepstad DC, Decarvalho CR, Davidson EA *et al*. (1994) The role of deep roots in the hydrological and carbon cycles of Amazonian forests and pastures. *Nature*, **372**, 666–669.

Nepstad DC, Lefebvre P, Da Silva UL *et al*. (2004) Amazon drought and its implications for flammability and tree growth: a basin wide analysis. *Global Change Biology*, **10**, 704–717.

Nepstad DC, Moutinho P, Dias MB *et al*. (2002) The effects of partial through-fall exclusion on canopy processes, above-ground production, and biogeochemistry of an Amazon forest. *Journal of Geophysical Research-Atmospheres*, **107**, 8085.

Newman EI (1969) Resistance to water flow in soil and plant I Soil resistance in relation to amounts of root: theoretical estimates. *Journal of Applied Ecology*, **6**, 1–12.

Ruivo MLP, Cunha ES (2003) Mineral and organic components in archaeological black earth and yellow latosol in Caxiuanã, Amazon, Brazil. In: *Ecosystems and Sustainable Development* (eds Tiezzi E, Brebbia CA, Usó JL), pp. 1113–1121. WIT Press, Southampton, UK.

Peylin P, Bousquet P, Le Quere C *et al*. (2006) Multiple Constraints on regional CO_2 flux variations over land and oceans. *Global Biogeochemical Cycle*, **19**, GB1011.

Potter CS, Davidson EA, Klooster SA, Nepstad DC, De Negreiros GH, Brooks V (1998) Regional application of an ecosystem production model for studies of biogeochemistry in Brazilian Amazonia. *Global Change Biology*, **4**, 315–333.

Prentice IC, Lloyd J (1998) C-Quest in the Amazon. *Nature*, **396**, 619–620.

Saleska SR, Miller SD, Matross DM, Goulden ML *et al*. (2003) Carbon in Amazon forests: unexpected seasonal fluxes and disturbance-induced losses. *Science*, **302**, 1554–1557.

Schellekens J, Scatena FN, Bruijnzeel LA, Wickel AJ (1999) Modelling rainfall interception by a lowland tropical rain forest in northeastern Puerto Rico. *Journal of Hydrology*, **225**, 168–184.

Smith KE, Mullins CE (2000) *Soil and Environmental Analysis: Physical Methods*. Marcel Dekker Inc., New York.

Sperry JS, Adler FR, Campbell GS, Comstock JP (1998) Limitation of plant water use by rhizosphere and xylem conductance: results from a model. *Plant, Cell and Environment*, **21**, 347–359.

Sperry JS, Hacke UG, Oren R, Comstock JP (2002) Water deficits and hydraulic limits to leaf water supply. *Plant, Cell and Environment*, **25**, 251–263.

Tian HQ, Melillo JM, Kicklighter DW, McGuire AD, Helfrich JVK, Moore B, Vorosmarty CJ (1998) Effect of interannual climate variability on carbon storage in Amazonian ecosystems. *Nature*, **396**, 664–667.

Tomasella J, Hodnett MG (1997) Estimating unsaturated hydraulic conductivity of Brazilian soils using soil water retention data. *Soil Science*, **162**, 703–712.

Tuzet A, Perrier A, Leuning R (2003) A coupled model of stomatal conductance, photosynthesis and transpiration. *Plant, Cell and Environment*, **26**, 1097–1116.

Tyree MT, Sperry JS (1988) Do woody-plants operate near the point of catastrophic xylem dysfunction caused by dynamic

water stress – answers from a model. *Plant Physiology*, **88**, 574–580.

Tyree MT, Velez V, Dalling JW (1998) Growth dynamics of root and shoot hydraulic conductance in seedlings of five neotropical tree species: scaling to show possible adaptation to differing light regimes. *Oecologia*, **114**, 293–298.

Ubarana VN (1996) Observation and modeling of rainfall interception at two rainforest sites in Amazonia. In: *Amazonian Deforestation and Climate* (eds Gash JHC, Nobre AD, Roberts JM, Victoria RL), pp. 55–77. Wiley, Chicester.

Van Genuchten MT (1980) A closed form equation for predicting hydraulic conductivity of unsaturated porous materials. *Soil Science Society of America Journal*, **44**, 892–898.

Veldkamp E, O'Brien JJ (2000) Calibration of a frequency domain reflectrometry sensor for humid tropical soils of volcanic origin. *Soil Science Society of America Journal*, **64**, 1549–1553.

Werth D, Avissar R (2004) The regional evapotranspiration of the Amazon. *Journal of Hydrometeorology*, **5**, 100–109.

Williams M, Bond BJ, Ryan MG (2001b) Evaluating different soil and plant hydraulic constraints on tree function using a model and sap flow data from ponderosa pine. *Plant, Cell and Environment*, **24**, 679–690.

Williams M, Eugster W, Rastetter EB, McFadden JP, Chapin FS (2000) The controls on net ecosystem productivity along an Arctic transect: a model comparison with flux measurements. *Global Change Biology*, **6**, 116–126.

Williams M, Law BE, Anthoni PM, Unsworth MH (2001a) Use of a simulation model and ecosystem flux data to examine carbon–water interactions in ponderosa pine. *Tree Physiology*, **21**, 287–298.

Williams M, Malhi Y, Nobre AD, Rastetter EB, Grace J, Pereira MGP (1998) Seasonal variation in net carbon exchange and evapotranspiration in a Brazilian rain forest: a modelling analysis. *Plant, Cell and Environment*, **21**, 953–968.

Williams M, Rastetter EB, Fernandes DN *et al*. (1996) Modelling the soil-plant-atmosphere continuum in a Quercus-Acer stand at Harvard forest: the regulation of stomatal conductance by light, nitrogen and soil/plant hydraulic properties. *Plant, Cell and Environment*, **19**, 911–927.

Williams M, Schwarz PA, Law BE, Irvine J, Kurpius M (2005) An improved analysis of forest carbon dynamics using data assimilation. *Global Change Biology*, **11**, 89–105.

Wong SC, Cowan IR, Farquhar GD (1979) Stomatal conductance correlates with photosynthetic capacity. *Nature*, **282**, 424–426.

Woodward FI, Lomas MR (2004) Vegetation dynamics – simulating responses to climate change. *Biological Review*, **79**, 643–670.

Zeng N, Mariotti A, Wetzel P (2005) Terrestrial mechanisms of interannual CO_2 variability. *Global biogeochemical cycles*, **19**, Art. No. GB1016.